Integrative Biology

Cite this: *Integr. Biol.*, 2012, **4**, 633–640

www.rsc.org/ibiology

PAPER

Synthetic curcumin analog EF31 inhibits the growth of head and neck squamous cell carcinoma xenografts

Shijun Zhu,[a] Terry W. Moore,[bc] Xiaoqian Lin,[a] Nao Morii,[a] Alessandra Mancini,[bc] Randy B. Howard,[b] Deborah Culver,[b] Richard F. Arrendale,[b] Prabhakar Reddy,[b] Taylor J. Evers,[b] Hongzheng Zhang,[a] Gabriel Sica,[d] Zhuo G. Chen,[a] Aiming Sun,[b] Haian Fu,[e] Fadlo R. Khuri,[a] Dong M. Shin,[a] James P. Snyder[bc] and Mamoru Shoji*[a]

Received 10th January 2012, Accepted 23rd March 2012
DOI: 10.1039/c2ib20007d

Objectives are to examine the efficacy, pharmacokinetics, and toxicology of a synthetic curcumin analog EF31 in head and neck squamous cell carcinoma. The synthesis of EF31 was described for the first time. Solubility of EF24 and EF31 was compared using nephelometric analysis. Human head and neck squamous cell carcinoma Tu212 xenograft tumors were established in athymic nude mice and treated with EF31 i.p. once daily five days a week for about 5–6 weeks. The long term effect of EF31 on the NF-κB signaling system in the tumors was examined by Western blot analysis. EF31 at 25 mg kg^{-1}, i.p. inhibited tumor growth almost completely. Solubilities of EF24 and EF31 are <10 and 13 μg mL^{-1} or <32 and 47 μM, respectively. The serum chemistry profiles of treated mice were within the limits of normal, they revealed a linear increase of C_{max}. EF31 decreased the level of phosphorylation of NF-κB p65. In conclusion, the novel synthetic curcumin analog EF31 is efficacious in inhibiting the growth of Tu212 xenograft tumors and may be useful for treating head and neck squamous cell carcinoma. The long term EF31 treatment inhibited NF-κB p65 phosphorylation in xenografts, implicating downregulation of cancer promoting transcription factors such as angiogenesis and metastasis.

Introduction

Curcumin (diferuloylmethane), a major component of turmeric, is used as a coloring and flavoring agent in many food items, including curries and mustard. Recent preclinical and clinical studies have demonstrated that this phytochemical has a number of anticancer properties.[1,2] The pharmacological safety of curcumin has been demonstrated by its consumption for centuries at levels of up to 100 mg per day by people in certain countries.[3] One problem with the clinical use of curcumin is its low potency and poor absorption characteristics;[4] however, curcumin remains an ideal lead compound for the design of more effective analogs. Using the shape and size of curcumin as a guide, we have designed and synthesized over 100 analogs. We and others have demonstrated that many of them are more potent than curcumin in a variety of cellular assays[5–9] and in animal models of disease.[10]

[a] *Department of Hematology and Medical Oncology, Winship Cancer Institute, Emory University, Atlanta, GA 30322, USA. E-mail: mshoji@emory.edu; Fax: +1 404 778 5016; Tel: +1 404 727 3457*
[b] *Emory Institute for Drug Discovery, Emory University, Atlanta, GA 30322, USA*
[c] *Department of Chemistry, Emory University, Atlanta, GA 30322, USA*
[d] *Department of Pathology, Emory University, Atlanta, GA 30322, USA*
[e] *Department of Pharmacology and Emory Chemical Biology Discovery Center, Emory University, Atlanta, GA 30322, USA*

Insight, innovation, integration

In this manuscript, we report the results of a study on a synthetic curcumin analog, EF31, its anti-tumor efficacy against xenografts of human squamous cell cancer Tu212, toxicologic studies, pharmacokinetic studies and effects on the NF-κB signaling system by a long term treatment of tumor xenografts. EF31 decreased NF-κB p65 phosphorylation by potentially inhibiting IKK-alpha and beta, and casein kinase II. We believe that our findings could be of interest to the readers of *Integrative Biology* because they bring to light a new curcumin analog and a possible mechanism for inhibiting tumor growth.

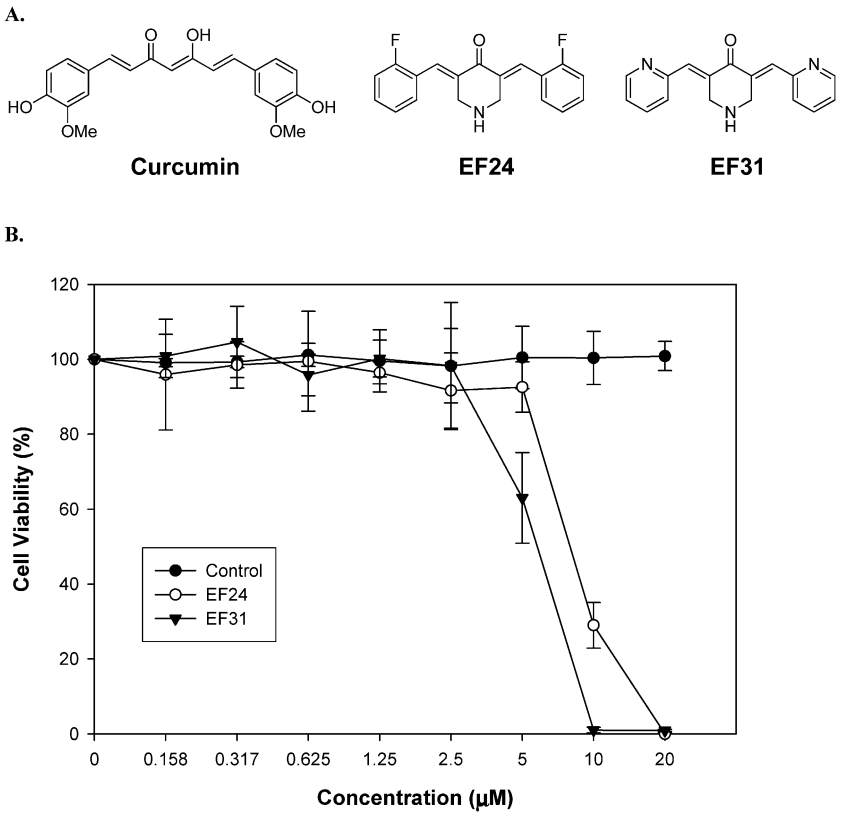

Fig. 1 Cytotoxic activity and solubility of EF24 and EF31 against Tu212 SCC cells *in vitro*. Chemical structures of curcumin, EF24, EF31 are shown. Molecular weights of curcumin, EF24 and EF31 are 368.38, 311.11, and 277.31 g mol^{-1}, respectively (Fig. 1A). Tu212 cells (10^4 cells per 0.2 mL per well) in a 96-well plate were incubated with varying doses of EF24, EF31 (0–20 μM) in triplicate for 48 hours. Viable cells were measured by Neutral Red Dye assay. IC_{50} values of EF24 and EF31 were 8 and 7 μM, respectively (Fig. 1B). The aqueous solubilities of EF24 and EF31 were determined by nephelometry to be <10 μg mL^{-1} (32 μM) and 13 μg mL^{-1} (47 μM), respectively. Solubilities of EF24 and EF31 are shown as the concentrations at which the solute began to precipitate out of solution and expressed as counts of refractive nephelometry units (RNU) (Fig. 1C).

One compound in particular, EF24 (Fig. 1), is more active than parent curcumin in its anticancer and antiangiogenesis effects.[5,6,10,11] The mechanism action of EF24, like curcumin, appears to involve multiple targets, the discovery of which is ongoing. We demonstrated that EF24 depolarizes the membrane potential of the mitochondrial membrane, causes G2/M arrest, activates caspase 3 and leads to apoptosis in human breast and prostate cancer cell lines.[6] Others have demonstrated that EF24 inhibits Akt and MDM2, an important negative regulator of the p53 tumor suppressor, by upregulating PTEN and enhancing the level of p53, thereby inducing G2/M arrest and apoptosis in human ovarian cancer cell lines.[12] EF24 significantly suppresses the growth of colon cancer tumor xenografts. In turn, these show decreased tumor angiogenesis, inhibition of Akt and ERK1/2 activation and reduced expression of COX-2, interleukin-8 and VEGF mRNA.[13]

NF-κB links to many cancers. Although such studies implicate NF-κB as a therapeutic target, mechanistically. To the extent it is known, curcumin and EF24 operate similarly in the NF-κB signaling pathway. Curcumin inhibits the NF-κB activation pathway at a step before IκBα phosphorylation.[14] The same group found that curcumin suppresses TNF-induced nuclear translocation of p65, which corresponds to the sequential suppression of IκBα kinase (IKK) activity, phosphorylation and degradation of IκBα, p65-phosphorylation, -nuclear translocation and -acetylation. Curcumin also inhibits TNF-induced Akt activation and its association with IKK. These results indicate that curcumin inhibits NF-κB activation and NF-κB regulated gene expression by inhibition of IKK and Akt activation.[15] Curcumin potently inhibits cytokine (TNF-α and/or IL-1β)-mediated NF-κB activation upstream of the NF-κB-inducing kinase (NIK) and its activation of the IKKα/IKKβ complex.[16] Curcumin reduces nuclear translocation of p65, induces apoptosis *in vitro* and attenuates hematogenous lung metastasis of human breast cancer MDA-MB-231 cells by intracardiac injection. These effects correlate with reduction of phosphorylated IκB and p65 by Western blot analysis.[17] EF24, as well as curcumin, suppresses the NF-κB signaling pathway through direct action on IKKβ and, thereby, inhibits nuclear translocation of p65.[8] Most of these observations are derived from short term treatment *in vitro*.

Our laboratory recently synthesized the curcumin analog EF31; and it is slightly more potent than EF24. Human Tu212 squamous cell carcinoma (SCC) xenografts in athymic nude mice were treated with EF31, intraperitoneally (i.p.), daily 5 days a week for over one month. EF31 exhibited dose-dependent suppression of tumor growth. In addition, we found decreased amounts of phosphorylated IKKβ and p65. Unexpectedly, increased amounts of phosphorylated IκBα were also detected by Western blot analysis. This is the first report of the anticancer activities of this compound *in vitro* and *in vivo*. We also report its

pharmacokinetic characteristics, its effects on serum chemistry in mice and the blockade of the NF-κB signaling pathways in tumors after being treated with the drugs for over a month.

Materials and methods

Synthesis of curcumin analog EF31

EF31 (3,5-bis(2-pyridinylmethylidene)-4-piperidone) was prepared by the following procedure. To a 250 mL round bottom flask (RBF) equipped with a stir bar was added 0.25 M aqueous sodium hydroxide (40 mL, 10 mmol). To this stirring base, were added 4-piperidone hydrochloride monohydrate (0.61 g, 4.0 mmol) and then 2-pyridinecarboxaldehyde (0.80 mL, 8.4 mmol). To the yellow solution was added 0.78 M acetyltrimethylammonium chloride (0.51 mL, 0.40 mmol), which gave an orange precipitate. After two hours an additional 0.13 g (0.31 eq. more) 2-pyridinecarboxaldehyde and 2 mL more 1 M NaOH (0.5 eq. more) were added. The reaction was allowed to stir at room temperature for 6 hours total. The reaction mixture was diluted with 40 mL of brine and then extracted with dichloromethane (DCM; 3 × 50 mL). The organic layer (bottom) was collected in a 250 mL Erlenmeyer flask. The yellow solution was dried over $MgSO_4$, filtered into a 500 mL RBF, concentrated *in vacuo* at ~400 mbar until a minimal amount of liquid remained, and then dried under high vacuum (mass balance: 1.64 g). The yellow solid was adsorbed onto silica and purified using column chromatography (0 to 20% MeOH in DCM; R_f = 0.43 in 10% MeOH in DCM) to give a yellow solid, which was further recrystallized from boiling absolute ethanol, to give 0.69 g (62% yield) of small yellow crystals. Mp 183–186 °C; TLC: 19 : 1 EtOAc–MeOH solvent system (R_f = 0.19); ^{1}H NMR (400 MHz, $CDCl_3$): δ (ppm) 8.68 (dd, J = 4.6, 0.9 Hz, 2H), 7.69 (td, J = 7.6, 1.8 Hz, 2H), 7.62 (s, 2H), 7.43 (d, J = 7.9 Hz, 2H), 7.18 (ddd, J = 7.6, 4.7, 1.1 Hz, 2H), 4.48–4.57 (m, 4H), 1.73 (br, s, 1H); ^{13}C NMR (100 MHz, $CDCl_3$): δ (ppm) 155.2, 149.9, 139.4, 136.5, 132.6, 127.7, 122.9, 48.8; HRMS-APCI (m/z): $[M + H]^+$ calculated for $C_{17}H_{16}N_3O$, 278.12879; found, 278.12888; analysis calculated for $C_{18}H_{17}N_3O$: C, 74.20; H, 5.88; N, 14.42%, and found: C, 74.09; H, 5.75; N, 14.42% (Scheme 1).

Nephelometry

A curcumin analog and an internal control were dissolved in 100% dimethyl sulfoxide (DMSO) to obtain a final concentration of 30 mg mL^{-1}. The 30 mg mL^{-1} stock solution was serially diluted (concentration profile: 30, 20, 15, 10, 7.5, 5, 2.5, 1.25, 0.63, 0.31, and 0.15 mg mL^{-1}) in test tubes with 100% DMSO. The concentration profile was transferred to 96 well microplates (Costar black clear bottom) and serially diluted to a final DMSO (EMD) concentration of 1% and a final drug concentration of 300, 200, 150, 100, 75, 50, 25, 12, 6, 3 and 1.5 μg mL^{-1} with phosphate buffered saline, pH 7.4 (Sigma).

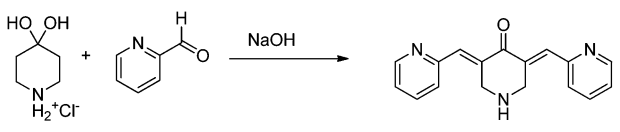

EF31

Scheme 1

The microplates were incubated for 90 minutes in the dark at ambient temperature. Laser nephelometry (NEPHELOstar, BMG Lab Technologies) was used to determine the point (concentration) at which the solute began to precipitate out of solution and expressed as counts of refractive nephelometry units (RNU). Laser nephelometry is the measurement of forward scattered light when a laser beam is directed through a solution.

Cell culture of Tu212 cells

Tu212 human SCC cells were maintained in DMEM/F12 (1 : 1) (Lonza, 12-719F) containing 10% fetal bovine serum (FBS) (Gibco, 26140-079), penicillin (100 units per mL), streptomycin (100 μg mL^{-1}) and 2 mM L-glutamine. Cells were incubated at 37 °C in 5% CO_2/95% air in a humid atmosphere.

Neutral red assay for cell viability to test the efficacy of EF31 treatment *in vitro*

This assay was carried out according to the methods published by a modification of the method of Zhang.[18] Tumor cells (Tu212) for the anticancer screen were plated at a concentration of 20 000 cells per 200 μL per well in a 96-well plate and incubated overnight to allow the cells to adhere. EF31 or vehicle (0.1% DMSO) (Sigma, St. Louis, MO) was then added to appropriate wells in various concentrations in triplicate. Subsequently, cells were incubated for 72 h. At the termination of culture, medium was removed and 200 μL of fresh, warm medium containing 50 μg of Neutral Red per mL (GIBCO-BRL, 15330-079, 0.33%) was added to each well. Cells were incubated at 37 °C for 30 min, followed by two washes with 200 μL of PBS. The Neutral Red taken up by cells was dissolved by adding 200 μL of 0.5 N HCl containing 35% ethanol. The plates were placed on a plate shaker until all residues were solubilized. Then, the amount of the dye in each well was read at 570 nm by a Universal Microplate Reader (EL800, Bio-Tek, Winooski, VT). Results from triplicate samples were recorded as optical density units (OD_{570}) and averaged after subtraction of the blank.

EF31 (i.p.) therapy *in vivo*

Nude mice were housed in a pathogen-free facility, and all procedures and protocols were approved by the Institutional Animal Care and Use Committee at Emory University. Tu212 cells (2 × 10^6 cells per mouse) were inoculated subcutaneously into the right posterior back of 7-week-old female athymic nude mice (nu/nu) mice (Harlan) and allowed to form a xenograft. When tumors reached a volume of approximately 150–200 mm^3, mice were randomized to receive either vehicle [0.5% carboxymethyl cellulose sodium (CMC) with 10% DMSO in sterile water] or drug (EF31). CMC was dissolved in distilled water and sterilized by autoclaving. Stock solution of the drugs was made fresh each time, weighing out EF31 (10 mg) and dissolved in 1 mL of 100% DMSO by brief heating before making appropriate dilution. EF31 was administered i.p. 5 days per week at a dosage of 12.5 or 25 mg kg^{-1}. Tumor size and body weights were measured twice a week. Tumor volume was calculated using the formula (width^2 × length)/2.

Pharmacokinetic studies

Male ND4 Swiss Webster mice (Harlan) weighing 25 to 30 g were used for the PK studies. Mice were each given a single dose of EF31 i.p. (12.5 or 25 mg kg^{-1}) in 10% DMSO/0.5% CMC. A single blood sample (0.3 mL) was taken from each animal under anesthesia (ketamine/xylazine, 100/10 mg kg^{-1}, s.c.) from the submandibular vein at one of eight different time points after dosing: 0.08, 0.25, 0.5, 1, 2, 3, 4 and 6 h ($n = 3$ mice per time point). Samples were collected in heparinized capillary tubes (Fisher), transferred to heparinized microtainers (BD) on ice in the dark and centrifuged within a few minutes at 2000 × *g* for five minutes in a refrigerated centrifuge to obtain plasma. Plasma was transferred to amber Eppendorf tubes (VWR) on ice, frozen for one hour and stored at −80 °C until analysis by LC/MS/MS within two days.

The plasma samples (50 μL) were deproteinated with acetonitrile (500 μL) and analyzed by LC/MS/MS using an internal standard spiking technique with an AB SCIEX 4000 QTRAP system equipped with an Agilent 1200 series HPLC using a developed and verified bioanalytical assay method to determine the plasma concentrations of EF31. The mean, standard deviation, and %CV of plasma levels were determined using Microsoft® Office Excel 2007. Mean concentration data were plotted against time to create plasma concentration *versus* time profiles.

Pharmacokinetic analysis of the plasma concentration data was conducted using non-compartmental analysis with WinNonlin Version 5.2.1. Areas under the curve (AUC) were estimated using the linear trapezoidal rule. The first order rate constant (Lambda Z) associated with the terminal (log-linear) elimination phase was estimated using linear regression of at least three non-zero concentrations *versus* time points in the late phase of the log concentration *versus* time profile. The half-life ($t_{1/2}$) was calculated as ln(2)/Lambda Z. Nominal times were used in all the data analysis.

Western blotting

Tumor tissue extracts were obtained by incubating tissue in RIPA buffer (50 mM Tris-HCl, pH 7.4, 1% NP-40, 0.25% sodium-deoxycholate, 150 mM NaCl, and 1 mM EDTA) supplemented with protease inhibitor cocktail (Complete; Roche) for 30 min on ice, then cleared by centrifugation at 13 000 rpm for 15 min at 4 °C. Total protein (100 μg) was separated by 10% SDS-PAGE gel and transferred onto polyvinylidene fluoride (PVDF) membranes (Hybond; GE Healthcare) for Western blotting. For Western blot detection, tissue extracts were boiled with 4 : 1 volume loading buffer. Primary antibodies for Western blotting were: IKKα (Cell Signaling Technology, #9936) at 1 : 1000, IKKα [phospho T23] (Abgent, AP3374a) at 1 : 1000, IKKβ (Novus, NB100-92040) at 1 : 1000, IKKβ [phospho Y199] (Abgent, AP3127a) at 1 : 500, NF-κB p65 (Novus, NB100-2176) at 1 : 1000, NF-κB p65 [phospho Ser276] (Novus, NB100-82086) at 1 : 1000, IκBα (Cell Signaling Technology, #4814) at 1 : 2000, IκBα [phospho Ser32/36] (Novus, NB100-92563) at 1 : 1000, or Actin (Santa Cruz Biotechnology, sc-1616) at 1 : 3000, anti-mouse IgG, anti-rabbit IgG, or anti-goat IgG horse radish peroxidase (HRP)-conjugated secondary antibodies (Cell Signaling Technology) were used at 1 : 5000, and HRP activity was visualized using the enhanced chemiluminescence (ECL) plus system (GE Healthcare).

Immunohistochemistry (IHC)

Tissues were fixed in 10% formaldehyde. After paraffin embedding, 6 μm sections were used for immunohistochemical studies. The paraffin-embedded sections of the tumor specimens were treated in xylene and dipped in a gradient of ethanol (once in 95% ethanol, once in 70% ethanol, once in 50% ethanol and once in water). The sections were heated in Tris-EDTA buffer (100 °C, 20 minutes). Endogenous peroxidase activity was blocked with 3% hydrogen peroxide. The sections were then incubated with a polyclonal antibody specific for each antigen. Primary antibodies were: IKKβ (Novus, NB100-92040) at 1 : 50, IKKβ [phospho Ser177/181] (USBio,13000-12) at 1 : 100, NF-κB p65 (Novus, NB100-2176) at 1 : 100, NF-κB p65 [phospho Ser276] (Novus, NB100-82086) at 1 : 100, IκBα (Cell Signaling Technology, 4814) at 1 : 50, IκBα [phospho Ser32/36] (Novus, NB100-92563) at 1 : 100. Incubation times were overnight at 4 °C. The sections were then incubated with anti-mouse and rabbit antibodies (abcam, ab64264; Mouse and Rabbit Specific HRP/DAB detection IHC kit), and the kit manufacturer's instructions were followed. Hematoxylin staining was used for histological diagnosis. Coverslips were mounted on glass slides with mounting medium. Controls using normal rabbit or rat serum were run to exclude nonspecific staining.

Statistical analysis

All the experiments in the study were repeated at least three times and the data are presented as the mean ± standard deviation. The significance of the difference between groups was evaluated with a two-tailed Student's *t*-test, $p < 0.05$ was considered significant.

Results

Cytotoxic activity and solubility of EF24, EF31

Cytotoxic activities in Tu212 SCC cells *in vitro* were assayed in triplicate using Neutral Red dye as described previously.[5,6] The IC_{50} values of EF24 and EF31 were similar with apparent IC_{50} values of 8 μM and 7 μM, respectively (Fig. 1A and B). The aqueous solubilities of EF24 and EF31 were determined by nephelometry to be <10 μg mL^{-1} (32 μM) and 13 μg mL^{-1} (47 μM) respectively.

Efficacy of EF31 in 0.5% CMC and 10% DMSO by i.p. injection into female athymic nude mice bearing Tu212 SCC xenografts

Animals bearing Tu212 SCC xenografts were treated with EF31 i.p. once daily for 5 days per week (M-F) with the following regimens, including the control group: Vehicle (0.5% CMC and 10% DMSO) ($n = 10$), Group 1: EF 31, 12.5 mg kg^{-1} (in vehicle) ($n = 10$), and Group 2: EF 31, 25 mg kg^{-1} (in vehicle) ($n = 10$). Asterisks indicate a significant difference in tumor size from the control ($p < 0.05$–0.01). Intraperitoneal administration provided the adequate plasma concentration of the drug to inhibit xenograft tumors. EF31 at 12.5 mg kg^{-1} and 25 mg kg^{-1} reduced the tumor size significantly, but the tumors continued to grow very slowly.

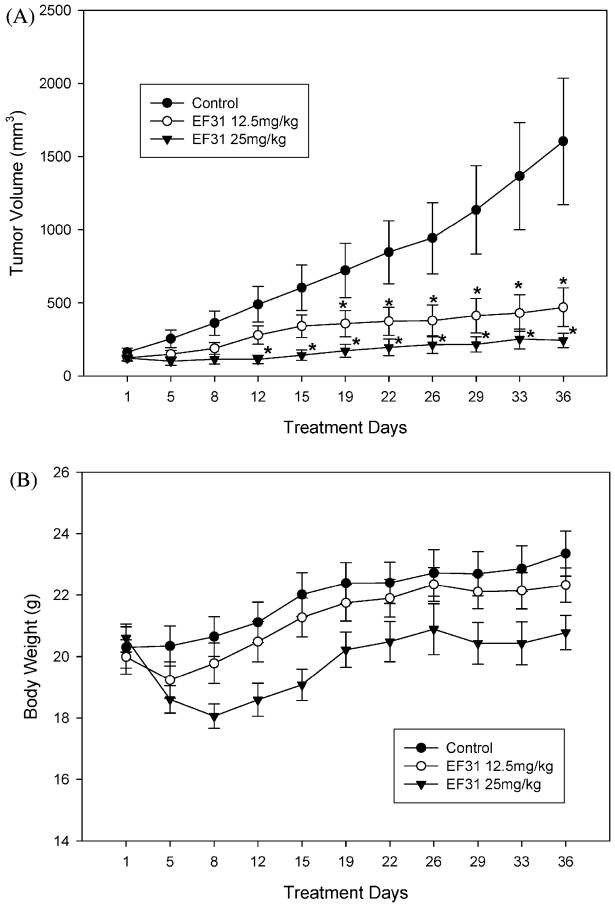

Fig. 2 Efficacy of EF31 in 0.5% carboxymethyl cellulose sodium (CMC) and 10% DMSO by i.p. in Tu212 SCC xenografts in female athymic nude mice. Tu212 cells (2×10^6 cells per 0.1 mL of medium) were inoculated subcutaneously (s.c.). EF31 (12.5 mg kg^{-1} and 25 mg kg^{-1}) or vehicle were administered intraperitoneally (i.p.) to mice ($n = 10$ per group) daily 5 days a week (Monday through Friday) for 5 weeks. Treatment was started when tumors grew to approximately 0.2–0.3 cm in diameter. (A) Tumor size. Asterisks indicate a significant difference from the control ($p < 0.05$–0.01). (B) EF31 at 25 mg kg^{-1} reduced body weight temporarily by ~10% on average but animals regained body weight as treatment continued.

Both doses of EF31 reduced body weight temporarily by ~10% during treatment days 7–11; however, the animals regained body weight upon continued treatment. In the EF31 (25 mg kg^{-1}) group, three animals died, apparently due to treatment. Thus, this i.p. dose may be above the maximally tolerated dose (MTD). Repeated experiments demonstrated similar efficacy for EF31 (Fig. 2A and B).

Effects on serum chemistry profiles and normal organs

The serum chemistry profile was within the normal values based on data from the University of Minnesota. Pathologic examination of hematoxylin–eosin staining of the liver, kidneys, lungs and spleen from six groups ($n = 5$ per group) including control, EF31 12.5 and 25 mg kg^{-1}, i.p. revealed normal. Analysis of serum chemistry revealed that both drugs significantly reduce alanine transaminase (ALT), alkaline phosphatase and phosphorus as compared with the controls, although even the lowest values are within the normal limits.

PK studies of EF31 in mice

After i.p. administration of EF31 at 12.5 and 25 mg kg^{-1} in a DMSO/0.5% CMC (10%/90%) formulation, peak mouse plasma concentrations were reached at 0.25 and 0.5 hours post-dose (T_{max}) with average concentrations (C_{max}) of 1067 and 2127 ng mL^{-1}, respectively. The terminal elimination half-life ($t_{1/2}$) averaged 2.2 and 2.4 hours, with an average AUC(0-∞) of 3386 and 7769 h × ng mL^{-1}, respectively. Following i.p. administration of EF31, the mean concentration *versus* time profiles suggested that the compound absorption rate was rapid and clearance from blood occurred at a moderate rate following C_{max} (Fig. 3A and B).

Both C_{max} and T_{max} in mice were dose proportional following i.p. administration of EF31 at 12.5 and 25 mg kg^{-1}. However, the terminal elimination half-lives ($t_{1/2}$) and volumes of distribution (Vz/F) were similar for both doses. The apparent terminal volumes of distribution (Vz/F) (corrected for weight) for EF31 were 11.5 and 11.1 L kg^{-1} for the 12.5 and 25 mg kg^{-1} doses, respectively. This may indicate a significant distribution of EF31 in total body water or tissues.

EF31 decreases the level of phosphorylated NF-κB p65

To explore the *in vivo* effects of EF31 on the NF-κB signaling pathway, we used Western blotting to analyze tumors from mice treated with EF31 at 12.5 mg kg^{-1} and 25 mg kg^{-1}, and vehicle control, i.p., for 6 weeks. This experiment was performed since the curcumin analog EF24 was demonstrated to inhibit NF-κB by inhibiting IκBα kinaseβ (IKKβ) *in vitro*.[8] EF31 at 25 mg kg^{-1} reduced the levels of phosphorylated IKKα but not the total IKKα as compared to the control. However, while the drug reduced the level of phosphorylated IKKβ, it also increased the level of total IKKβ in a dose-dependent manner. Levels of the down-stream target of IKKβ, IκBα phosphorylated at serine 32 and 36, were increased, but the total IκBα decreased in a dose-dependent manner. EF31 decreased the levels of both the phosphorylated NF-κB p65 at Ser276 as measured and the total p65 in a dose-dependent manner (Fig. 4).

In the hematoxylin and eosin (H&E) staining experiments, tumor tissues treated at 25 mg kg^{-1} are almost entirely replaced with pink, ring-shaped structures that surround a small nest of tumors in the center. It appears that the tumor cells are replaced with fibrous scar tissue (Fig. 5). The rank order of the degree of the IHC staining of the phosphorylated IκBα is stronger in tumors treated at 25 mg kg^{-1} than 12.5 mg kg^{-1}, which is stronger than that in the control (Fig. 5). All of IKKβ, phosphorylated IKKβ, IκBα, phosphorylated IκBα, NF-κB p65 and phosphorylated NF-κB p65 results correspond with that of the Western blot (Fig. 4 and 5). In an *in vitro* short term culture of cells treated with cytokines, it is likely that phosphorylated IκBα will be decreased in the presence of EF31.[30]

Discussion

In this report, we demonstrate that the synthetic curcumin analog EF31 significantly inhibits the growth of human head

A. EF31 administered by i.p.

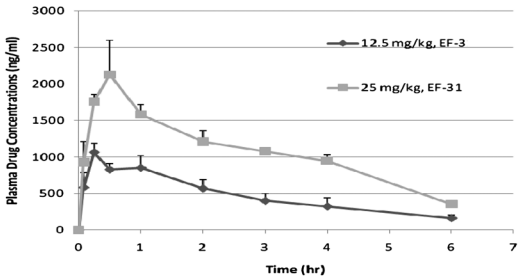

B. Calculated pharmacokinetic parameters of EF31, i.p. at 12.5 and 25 mg/kg.

Dose (mg/kg)	T_{max} (hr)	C_{max} (ng/mL)	T½ (hr)	AUC (0-t) (hr*ng/mL)	AUC (0-∞) (hr*ng/mL)	AUC % Extrap	Vz_F (L/kg)
12.5	0.25	1067	2.2	2876	3386	15	11.5
25	0.50	2127	2.4	6545	7769	15.8	11.1

Fig. 3 Pharmacokinetic study of EF31 administered i.p. (A, B) After i.p. administration of EF31 at 25 mg kg^{-1} in a DMSO/0.5% CMC (10%/90%) formulation, peak mouse plasma concentrations were reached at 0.5 hours post-dose (T_{max}) with an average concentration (C_{max}) of 2127 ng mL^{-1}. The terminal elimination half-life ($t_{1/2}$) averaged 2.4 hours, with an average AUC(0-∞) of 7769 h × ng mL^{-1}. Both C_{max} and T_{max} were dose proportional following i.p. administration of EF31 to mice at 12.5 and 25 mg kg^{-1}.

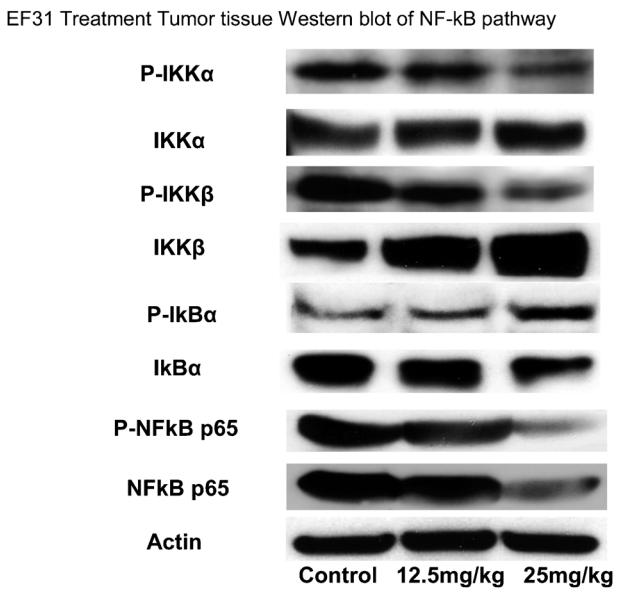

Fig. 4 Changes in the NF-κB pathways in tumors treated with EF31 (Western blots). Tumor bearing animals were treated with EF31 0, 12.5 mg kg^{-1} and 25 mg kg^{-1} i.p. daily 5 days a week for 5 weeks as shown in Fig. 2. Tumor extracts were analyzed by Western blotting using various antibodies for NF-κB pathways.

and neck squamous cell cancer xenografts. The drug was efficacious when formulated in 0.5% CMC and 10% DMSO.

A pharmacokinetic (PK) study was done in mice to characterize the drug levels and PK parameters associated with i.p. dosing of EF-31 under the conditions that were used in the tumor efficacy experiment (Fig. 2). Examination of the results shows that peak plasma levels were reached within 30 minutes and that measurable drug levels were seen for at least six hours. Both C_{max} and AUC were dose-related, with the C_{max} values falling in the 1 to 2 μg mL^{-1} range, consistent with the micromolar drug concentrations (4–8 μM) that were required for tumor cell growth inhibition *in vitro* (Fig. 1). Estimated volumes of distribution were ~11 L kg^{-1}, suggesting significant penetration of tissues. Several factors might influence the efficacy of EF31, including IC_{50} values, the aqueous solubility, and the terminal elimination half-life ($t_{1/2}$) of EF31 12.5 and 25 mg kg^{-1}, which averaged 2.2 and 2.4 hours.

Western blot analyses were performed on Tu212 tumor xenografts from animals treated for 6 weeks with EF31. The results reflect the effects of long-term drug treatment on the NF-κB signaling pathway, in contrast to short term treatment (hours) of cells *in vitro*. EF24, an analog of EF31, was previously shown to inhibit IKKβ activity by means of TNF-α induced IκBα phosphorylation during short term incubation (30 min–3 h) *in vitro*.[8]

The level of p-IKKα and p-IKKβ decreased in a dose-dependent manner, whereas the level of unphosphorylated IKKα and IKKβ increased in a dose-dependent manner. This reciprocal response of tumors to a long-term treatment of EF31 dose at 0, 12.5, and 25 mg kg^{-1} may suggest a compensatory reaction of tumors to the inhibition of IKKα and IKKβ phosphorylation. The reciprocal response in the level of increased p-IκBα and the level of decreased unphosphorylated IκBα in a dose-dependent manner is also seen but this is counterintuitive, since the levels of both p-IKKα and p-IKKβ that phosphorylate IκBα were decreased. This suggests the presence of other IκBα kinases that phosphorylate IκBα, leading to the process of ubiquitination, degradation of IκBα. This degradation of IκBα from the IκBα/NF-κB p65–p50 complex promotes the increased nuclear translocation of NF-κB p65–p50. The IκB kinases IKKα/β complex,

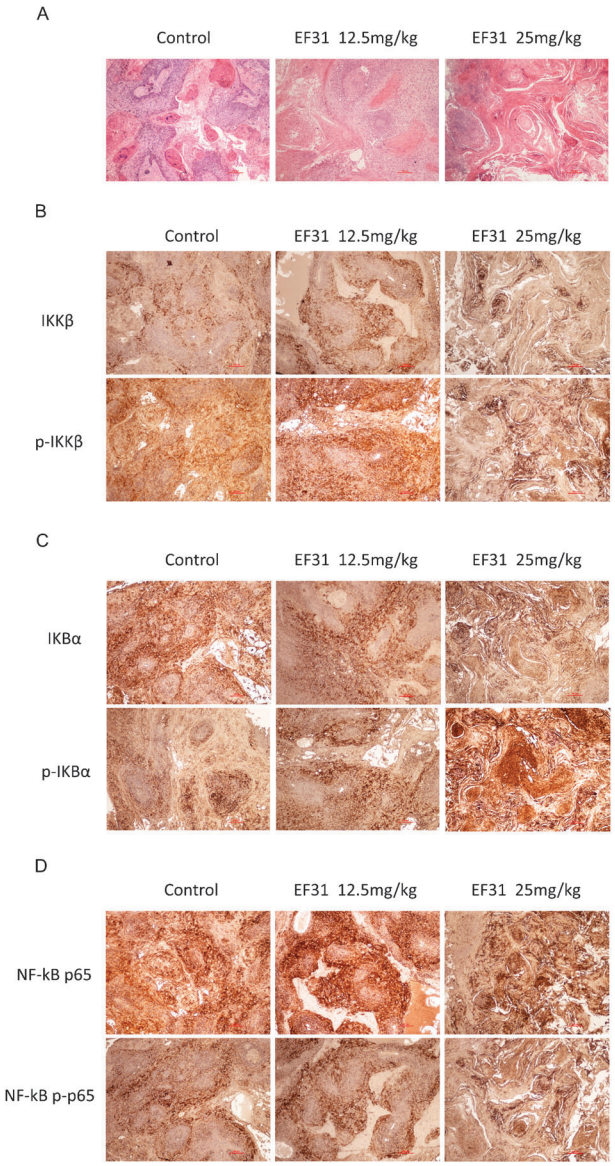

Fig. 5 Hemotoxylin and eosin staining (×100) and corresponding immunohistochemistry patterns of xenografts mouse tumor tissues. (A) H&E staining, tumor bearing animals were treated with EF31 0, 12.5 mg kg^{-1} and 25 mg kg^{-1} i.p. daily 5 days a week for 5 weeks. (B) IKKβ and phospho-IKKβ staining of mice tumor tissues serial sections. (C) IκBα and phospho-IκBα staining of mice tumor tissues serial sections. (D) NF-κB p65 and NF-κB phospho-p65 staining of mice tumor tissues serial sections. The scale bars indicate 100 μm.

casein kinase II (CKII), and the mitogen-activated 90 kDa ribosomal S6 kinase (p90rsk1) can phosphorylate one or both of the two serines (Serine 32 and Serine 36) in IκBα.[19] Inhibition of CKII significantly suppressed tumor growth in HNSCC xenograft models.[20] EF31 inhibited HNSCC xenografts, suggesting that EF31 also inhibited CKII. It is unknown whether EF31 inhibits the p90rsk1. Thus, there are two potential candidates that increased the level of the phosphorylated IκBα. First, it has been demonstrated that the p38 MAPK stimulated by transforming growth factor (TGF)-β1 phosphorylated IκBα.[21] Since EF24 does not inhibit p38 MAPK activity,[9] it is unlikely that EF31 inhibits the p38 MAPK. Second, tyrosine phosphorylation of IκBα activated NF-κB without proteolytic degradation of IκBα.[22] Western blot analysis revealed that the levels of both phosphorylated NF-κB p65 and unphosphorylated NF-κB p65 were decreased in an EF31 dose-dependent manner. The mechanism of homeostatic maintenance of the NF-κB level is well documented. NF-κB (*e.g.*, p65–p50 heterodimer) binds to the κB site on the promoter region of IκBα and induces its re-synthesis.[23] The newly synthesized IκBα is translocated into the nucleus, where it binds and transports NF-κB to the cytoplasm.[24] The autoregulatory loop between NF-κB and IκBα is responsible for maintenance of the homeostasis of NF-κB and IκBα. We demonstrated that EF31 decreased the level of total IκBα, and the level of phosphorylated and total p65 NF-κB in a relatively dose-dependent manner. It is unclear why the phosphorylated IκBα was present abundantly in the fibrous structure by the IHC staining. It could be that in the process of continuous chemotherapy with EF31, the tumor cells are nearly dead and cannot produce the adequate levels of ubiquitin-proteasome to degrade the phosphorylated IκBα, leaving it to be absorbed and deposited onto the continuously growing, fibrous scar tissue in the tumors.

NF-κB p65 is phosphorylated at serine 276 (p-NF-κB p65), the major site of phosphorylation. Two protein kinases phosphorylate NF-κB p65 at serine 276. These are the catalytic subunit (PKAc) of cyclic AMP-dependent protein kinase (A-PK)[25,26] and mitogen- and stress-activated protein kinase (MSK1), which is a kinase activated in cells downstream of both the ERK1/2 (extracellular-signal-regulated kinase) and p38 MAPK (mitogen-activated protein kinase) cascades.[27,28] Inhibition of MSK1 by EF31 is unlikely because EF24 was demonstrated to increase phosphorylation of ERK1/2, JNK and p38.[9] Thus, it is possible that EF31 inhibits PKAc in tumors undergoing chronic treatment. Indeed, curcumin was shown to inhibit PKAc.[29]

Conflict of interest: none declared.

Grant support

This research was supported by the National Cancer Institute award 5 P50 CA128613 SPORE in Head and Neck Cancer (SZ, TWM, HZ, XL, GC, HF, FRK, DMS, JPS, MS), the National Institutes of Health (NIH) grant R21CA82995-01A1, the U.S. Department of Defense, Division of U.S. Army DAMD17-00-1-0241 (MS), and the Emory Institute for Drug Discovery (TWM, AM, RBH, DC, RFA, GRP, TJE, AS, JPS).

Acknowledgements

We gratefully acknowledge Dr Anthea Hammond, PhD, for correcting the manuscript.

References

1 B. B. Aggarwal, A. Kumar and A. C. Bharti, Anticancer potential of curcumin: preclinical and clinical studies, *Anticancer Res.*, 2003, **23**, 363–398.
2 M. M. Chaturvedi, B. Sung, V. R. Yadav, R. Kannappan and B. B. Aggarwal, NF-κB addiction and its role in cancer: 'one size does not fit all', *Oncogene*, 2011, **30**, 1615–1630.
3 R. R. Satoskar, S. J. Shah and S. G. Shenoy, Evaluation of anti-inflammatory property of curcumin (diferuloylmethane) in patients

with post-operative inflammation, *Int. J. Clin. Pharmacol., Ther. Toxicol.*, 1986, **24**, 651–654.
4 G. Shoba, D. Joy, T. Joseph, M. Majeed, R. Rajendran and P. S. Srivinas, Influence of piperine on the in animals pharmacokinetics of curcumin and human volunteers, *Planta Med.*, 1998, **64**, 353–356.
5 B. K. Adams, E. M. Ferstl, M. C. Davis, M. Herold, S. Kurtkaya and R. F. Camalier, *et al.* Synthesis and biological evaluation of novel curcumin analogs as anti-cancer and anti-angiogenesis agents, *Bioorg. Med. Chem.*, 2004, **12**, 3871–3883.
6 B. K. Adams, J. Cai, J. Armstrong, M. Herold, Y. J. Lu and A. Sun, *et al.* EF24, a novel synthetic curcumin analog, induces apoptosis in cancer cells *via* a redox-dependent mechanism, *Anticancer Drugs*, 2005, **16**, 263–275.
7 I. Landais, S. Hiddingh, M. McCarroll, C. Yang, A. Sun and M. S. Turker, *et al.* Monoketone analogs of curcumin, a new class of Fanconi anemia pathway inhibitors, *Mol. Cancer*, 2009, **8**, 133–145.
8 A. L. Kasinski, D. Yuhong, S. L. Thomas, J. Zhao, S. Y. Sun and F. Khuri, *et al.* Inhibition of IKK-NF-kappa B signaling pathway by EF24, a novel monoketone analogue of curcumin, *Mol. Pharmacol.*, 2008, **74**, 654–661.
9 S. L. Thomas, J. Zhao, Z. Li, B. Lou, Y. Du and J. Purcell, *et al.* Activation of the p38 pathway by a novel monoketone curcumin analog, EF24, suggests a potential combination strategy, *Biochem. Pharmacol.*, 2010, **80**, 1309–1316.
10 M. Shoji, A. Sun, W. Kisiel, Y. J. Lu, H. Shim and B. E. McCarey, *et al.* Targeting therapy of tumor angiogenesis with a novel synthetic curcumin analog EF24 conjugated to factor VIIa inhibitor, *J. Drug Targeting*, 2008, **16**, 185–197.
11 A. Sun, M. Shoji, J. P. Snyder and D. C. Liotta, Synthesis of EF24-tripeptide-chloromethylketone: A novel anti-cancer drug delivery system, *J. Med. Chem.*, 2006, **49**, 3153–3158.
12 K. Selvendiran, L. Tong, S. Vishwanath, A. Bratasz, N. J. Trigg and V. K. Kutala, *et al.* EF24 induces G2/M arrest and apoptosis in cisplatin-resistant human ovarian cancer cells by increasing PTEN expression, *J. Biol. Chem.*, 2007, **282**, 28609–28618.
13 D. Subramaniam, R. May, S. M. Sureban, K. B. Lee, R. George and P. Kuppusamy, *et al.* A Curcumin Derivative with Potent *In vivo* Anticancer Activity, *Cancer Res.*, 2008, **68**, 1962–1969.
14 S. Singh and B. B. Aggarwal, Activation of transcription factor NF-κB is suppressed by curcumin (diferuloylmethane), *J. Biol. Chem.*, 1995, **270**, 24995–25000.
15 S. Aggarwal, H. Ichikawa, Y. Takada, S. K. Sandur, S. Shishodia and B. B. Aggarwal, Curcumin (diferuloylmethane) down-regulates expression of cell proliferation and antiapoptotic and metastatic gene products through suppression of IkappaBalpha kinase and Akt activation, *Mol. Pharmacol.*, 2006, **69**, 195–206.
16 C. Jobin, C. A. Bradham, M. P. Russo, B. Juma, A. S. Narula and D. A. Brenner, *et al.* Curcumin blocks cytokine-mediated NF-kappa B activation and proinflammatory gene expression by inhibiting inhibitory factor Ikappa B kinase activity, *J. Immunol.*, 1999, **163**, 3474–3483.
17 B. E. Bachmeier, A. G. Nerlich, C. M. Iancu, M. Cilli, E. Schleicher, R. Vené, R. Dell'Eva and M. Jochum, The chemopreventive polyphenol curcumin prevents hematogenous breast cancer metastases in immunodeficient mice, *Cell. Physiol. Biochem.*, 2007, **19**, 137–152.
18 S. Z. Zhang, M. M. Lipsky, B. F. Trump and I. C. Hsu, Neutral red (NR) assay for cell viability and xenobiotic-induced cytotoxicity in primary cultures of human and rat hepatocytes, *Cell Biol. Toxicol.*, 1990, **6**, 219–234.
19 R. Heilker, F. Freuler, R. Pulfer, F. Di Padova and J. Eder, All three IκB isoforms and most Rel family members are stably associated with the IkB kinase 1/2 complex, *Eur. J. Biochem.*, 1999, **259**, 253–261.
20 M. S. Brown, O. T. Diallo, M. Hu, R. Ehsanian, X. Yang and P. Arun, *et al.* CK2 modulation of NF-kappaB, TP53, and the malignant phenotype in head and neck cancer by anti-CK2 oligonucleotides *in vitro* or *in vivo via* sub-50-nm nanocapsules, *Clin. Cancer Res.*, 2010, **16**, 2295–2307.
21 J. I. Park, M. G. Lee, K. Cho, B. J. Park, K. S. Chae and D. S. Byun, *et al.* Transforming growth factor-β1 activates interleukin-6 expression in prostate cancer cells through the synergistic collaboration of the Smad2, p38-NF-κB, JNK, and Ras signaling pathways, *Oncogene*, 2003, **22**, 4314–4332.
22 V. Imbert, R. A. Rupec, A. Livolsi, H. L. Pahl, E. B. Traenckner and C. Mueller-Dieckmann, *et al.* Tyrosine Phosphorylation of IkB-α Activates NF-κB without Proteolytic Degradation of IkB-α, *Cell*, 1996, **86**, 787–798.
23 P. J. Chiao, S. Miyamoto and I. M. Verma, Autoregulation of IκBα activity, *Proc. Natl. Acad. Sci. U. S. A.*, 1994, **91**, 28–32.
24 F. Arenzana-Seisdedos, P. Turpin, M. Rodriguez, D. Thomas, R. T. Hay, J. L. Virelizier and C. Dargemont, Nuclear localization of IκBα promotes active transport of NF-κB from the nucleus to the cytoplasm, *J. Cell Sci.*, 1997, **110**, 369–378.
25 H. Zhong, H. SuYang, H. Erdjument-Bromage, P. Tempst and S. Ghosh, The transcriptional activity of NF-kB is regulated by the IκB-associated PKAc subunit through a cyclic AMP-independent mechanism, *Cell*, 1997, **89**, 413–424.
26 C. Yoon, Z. Korade and B. D. Carter, Protein kinase A-induced phosphorylation of the p65 subunit of nuclear factor-κB promotes Schwann Cell differentiation into a myelinating phenotype, *J. Neurosci.*, 2008, **28**, 3738–3746.
27 M. Deak, A. D. Clifton, J. M. Lucocq and D. R. Alessi, Mitogen- and stress-activated protein kinase-1 (MSK1) is directly activated by MAPK and SAPK2/p38, and may mediate activation of CREB, *EMBO J.*, 1998, **17**, 4426–4441.
28 K. Kefaloyianni, C. Gaitanaki and I. Beis, ERK1/2 and p38-MAPK signalling pathways, through MSK1, are involved in NF-κB transactivation during oxidative stress in skeletal myoblasts, *Cell. Signalling*, 2006, **18**, 2238–2251.
29 M. Hsameda and G. M. Polya, Inhibition of cyclic AMP-dependent protein kinase by curcumin, *Phytochemicals*, 1996, **42**, 599–605.
30 A. Olivera, T. W. Moore, F. Hu, A. P. Brown, A. Sun and D. C. Liotta, *et al.*, Inhibition of the NF-κB signaling pathway by the curcumin analog, 3,5-bis(2-pyridinylmethylidene)-4-piperidone (EF31): Anti-inflammatory and anti-cancer properties, *Int. Immunopharmacol.*, 2012, **12**, 368–377.

